Analysis on Stick and Slip Behavior of Cleaning Blades

*Kuniki Seino, Shizuo Yuge and Masao Uemura**
Minolta Co., Ltd., Toyokawa, Aichi, Japan
**Toyohashi University of Technology, Toyohashi, Aichi, Japan*

Abstract

We have previously reported that in a leading-type blade cleaning systems for electrophotography, the lifetime of cleaning blades depends on the rebound resilience (R) of polyurethane rubber.[1] In this paper, we examine the general profile of the cleaning performance (cleaning ability and lifetime of cleaning blades) in terms of the stick-slip behavior of the cleaning blade. The rate of abrasion α is defined as wear volume per unit friction length. A theoretical analysis of fatigue wear shows that α is inversely proportional to the product, $N_0 L_0$, of the number (N_0) of friction vibrations stripping off small fragments of polyurethane rubber and the friction length (L_0) per one cycle of vibration. Laboratory tests for fatigue fracture of polyurethane rubber show that N_0 is proportional to the $-$ m-th power of ($\mu W^{0.47}$), where μ is the friction coefficient and W is the weight of the cleaning blade onto the photoreceptor surface. The cleaning blade edge has a stick-slip behavior against the surface of the photoreceptor. A new model, which takes into account viscoelastic behavior, is applied to the friction length. A cleaning blade edge once stretched by photoreceptor surface contracts with a relaxation time τ during the slip motion and $L_0 \propto -\ln R$ is deduced. During the slip process, the blade forces remaining toner particles to move against rotating direction of photoconductive drum. It encounters greater possibility of toner particles going through blade nip during the slip processes. Therefore, the cleaning ability is proportional to $1/L_0$ i.e. $-1/\ln R$.

Introduction

A blade cleaning method is widely used in electro-photographic copiers and printers. However, there is still a strong demand for better cleaning ability and longer lifetime of the cleaning blade. Toner has been made increasingly fine in diameter and the maintenance free is of urgent necessity. We examine the general profile of the cleaning performance (cleaning ability and lifetime of cleaning blades) in terms of the stick-slip behavior of the cleaning blade.

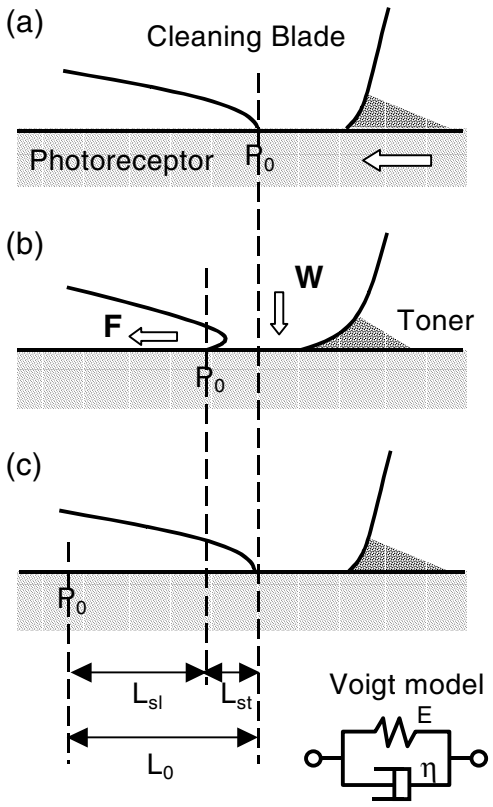

Figure 1. A stick-slip cycle governed by viscoelastic properties of cleaning blades. W and F indicate weight onto the photoreceptor surface and friction force for the cleaning blade respectively. (a)→ (b) : stick process. Position P_0 on the photoreceptor surface moves by L_{st}. (b) → (c) : slip process. Position P_0 moves by L_{sl} while the cleaning blade edge contracts with a relaxation time during slip motion. L_0 : friction length per one cycle of the stick-slip. L_{st} : stick length. L_{sl} : slip length.

Wear Characteristics of Cleaning Blade

Mechanism of Wear

Figure 1 gives a conceptual view of stick-slip behavior of a cleaning blade. When a blade nip sticks on a

photoreceptor surface, it is stretched in the direction towards which a photoreceptor layer moves (Fig. 1(a) → (b)). Repulsive force of the cleaning blade increases in proportion to stretched length of the blade edge. When the repulsive force reaches static friction force between the blade nip and the photoreceptor surface, the blade edge begins sliding and returns to its original position because the coefficient of kinetic friction is smaller than that of static one (Fig. 1 (b) → (c)). The repeated cycles of stick-slip motion force the blade edge to be worn out by fatigue, stripping off small fragments of polyurethane rubber.

Consider the cleaning blade with worn surface width of z as shown in Fig. 2. For simplicity, assuming that worn particles are cubes of $u \times u \times u$ and the surface is worn uniformly, the number of total worn particles generated is z/u. Also, the total number of friction vibrations necessary to wear the thickness by u is $N_0 \times z/u$, where N_0 is the number of friction vibrations for generating one worn particle. Then, the unit friction length L_u necessary to wear the thickness by u can be expressed as follows:

$$L_u = N_0 L_0 z / u \tag{1}$$

where L_0 is the friction length per one cycle of the stick-slip. Therefore, the worn height per unit friction length is given by

$$u / L_u = u^2 / N_0 L_0 z \tag{2}$$

Now suppose the worn height h in Fig. 2 increases continuously with the sliding distance l of the blade edge on the photoreceptor surface. Based on Eq. 2, an infinitely small worn volume Δh per an infinitely small sliding length Δl can be expressed as,

$$\Delta h / \Delta l = u^2 / N_0 L_0 z = \sin\theta \cos\theta \, u^2 / N_0 L_0 h \tag{3}$$

where the angle θ is defined in Fig. 2. Then, in the limit when Δl approaches 0,

$$dh / dl = \sin\theta \cos\theta \, u^2 / N_0 L_0 h \tag{4}$$

When $\alpha = u^2/N_0L_0$ is defined as wear volume per unit friction length, Eq. 4 can be expressed as,

$$dh / dl = \sin\theta \cos\theta \, \alpha / h \tag{5}$$

Friction Coefficient of Cleaning Blade

The experimental arrangement of a laboratory tester for friction between cleaning blades and the photoreceptor surface is identical to a blade cleaning apparatus shown in Fig. 5. The cleaning blade is pressed to the photoconductive drum and the weight is measured by a loadcell. The friction force is measured by a torque-meter connected to the drum axis. The observation is the average coefficient of static and kinetic friction because both the stick and slip behavior influence.

The contact area is observed by replacing the photoconductive drum with a glass cylinder of the same diameter containing a CCD camera inside. The following relation between the apparent contact area A_n and the weight W is obtained.

$$A_n = 46\, W^{0.53} \tag{6}$$

Assuming that the apparent contact area A_n is equal to the real contact area A_r, the friction force is given by

$$F = \tau_{AB} A_n \tag{7}$$

where τ_{AB} is the average shear strength. The substitution of Eq. 7 into Eq. 6 yields the coefficient of friction μ as,

$$\mu = F/W = 46\, \tau_{AB} / W^{0.47} \tag{8}$$

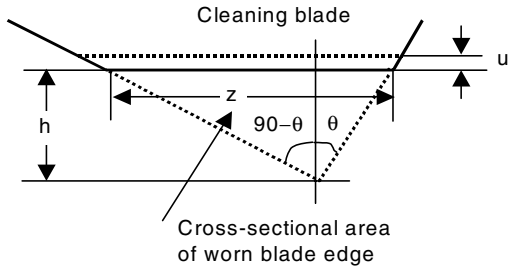

Figure 2. Worn surface width and cross-sectional area of worn blade edge.

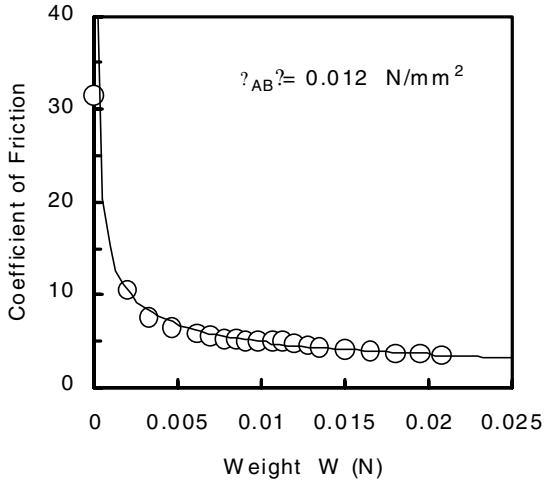

Figure 3. Typical example of relationship between coefficient of friction and weight for polyurethane blade at the photoreceptor surface. The solid curve is calculated from Eq. 8 with τ_{AB} = 0.012 N/mm^2.

The results of measurements are shown in Fig. 3. The good agreement with the curve calculated using Eq. 8 with τ_{AB} = 0.012 N/mm^2 indicates that shear strength is constant regardless of weight or pressure.

Friction vibrations

The laboratory test regarding fatigue was carried out in order to investigate the mechanism of fatigue wear1. The sample No. 8 in Table 1 was tested at 25°C and 50°C. Based on the results shown in Fig. 4, the reciprocal of repeated cycles to life N_c is found to relate to the stress σ as,

$$1 / N_c \propto \sigma^m \tag{9}$$

where m=6.5 at 25 °C and m=7.0 at 50 °C. Because N_c and the stress are likely to be proportional to N_0 and the average shear strength τ_{AB}, respectively, Eq. 9 can be rewritten as,

$$1 / N_0 \propto \sigma^m \propto \tau_{AB}^{\ m} \tag{10}$$

Substituting τ_{AB} from Eq. 8, we have,

$$N_0 \propto \tau_{AB}^{-m} \propto (\mu\, W^{0.47})^{-m} \tag{11}$$

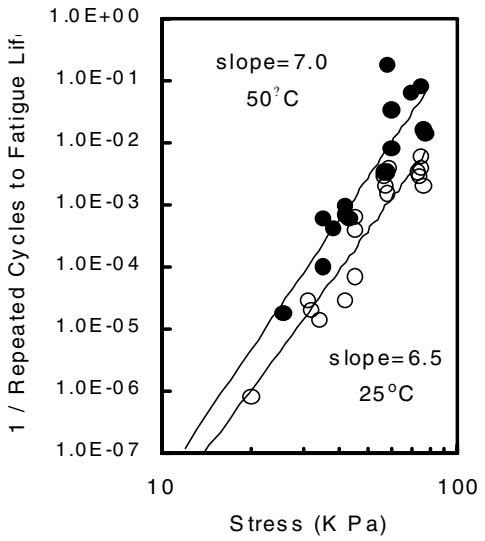

Figure 4. The reciprocal of repeated cycles to life as a function of stress to polyurethane rubber.

Friction Length

As shown in Fig. 1 the friction length L_0 per one cycle of vibration is given by the following equation:

$$L_0 = L_{st} + L_{sl} \tag{12}$$

where L_{st} is the stick length and L_{sl} is the slip length. P_0 moves by L_{sl} during the slip process.

We apply the Voigt model to the stick-slip behavior of cleaning blades shown in Fig. 1. During the stick process the repulsive force increases in proportion to stretched length γ of the blade edge. When the repulsive force reaches the static friction force F_s (=$\mu_s W$), relative sliding results between the photoreceptor surface and the blade nip. Assuming $\gamma = \gamma_0$ at this point, we have,

$$F_s = E\,\gamma_0 = \mu_s\, W \tag{13}$$

The blade nip returns to its original position gradually with relaxation time, and the stretched length γ during slip process can be expressed by the following equation:

$$F_k = E\,\gamma + \eta\, d\gamma / dt \tag{14}$$

where F_k is the kinetic friction force and η is the viscosity. The general solution of Eq. 14 is given by

$$\gamma = F_k/E + C \exp(-t/\tau) \tag{15}$$

where τ (= η/E) is the relaxation time. The stretched length contracts until the repulsive force equals to the kinetic friction force F_k (=μ_kW). Denoting γ at this point as γ_k, we have,

$$Fk = E\,\gamma k = \mu k\, W \tag{16}$$

Assuming Eq. 13 at t = 0 and Eq. 16 at t = ∞, Eq. 15 leads to Eq. 17 and Eq. 18

$$\gamma = \gamma_k + (\gamma_0 - \gamma_k) \exp(-t/\tau) \tag{17}$$

$$t = \tau \ln \{(\gamma_0 - \gamma_k) / (\gamma - \gamma_k)\} \tag{18}$$

When the repulsive force decays to any friction force, the blade nip sticks on the photoreceptor. However it takes infinite time to reach the kinetic friction force as indicated by Eq. 18. Actually, however, the kinetic friction force increases during the slip process, because the blade edge is compressed at its original position. Expressing the incremental friction force with the incremental friction coefficient μ_δ, and assuming that the blade nip sticks on the photoreceptor surface again when γ decays to $\gamma_k + \mu_\delta W/E$, the substitution of Eq. 13 and Eq. 16 into Eq. 18 yields the slip time t_{sl} as

$$t_{sl} = \tau \ln \{(\mu_s - \mu_k) / \mu_\delta\} \tag{19}$$

Therefore, the slip length L_{sl} can be given by

$$L_{sl} = v\, t_{sl} = v\, \tau\, n \{(\mu_s - \mu_k) / \mu_\delta\} \tag{20}$$

where v is the rotating velocity of the photoconductive drum. The stick length can be expressed as follows:

$$L_{st} = \gamma_0 - (\gamma_k + \mu_\delta W/E) = (\mu_s - \mu_k - \mu_\delta)\, W/E \tag{21}$$

The substitution of Eq. 20 and 21 into Eq. 12 yields the friction length as

$$L_0 = (\mu_\sigma - \mu_\kappa - \mu_\delta)\, W/E + v\, \tau \ln \{(\mu_s - \mu_k) / \mu_\delta\} \tag{22}$$

The relationship between rebound resilience and the vibration loss tan δ is given by

$$R = \exp(-\pi \tan \delta) \tag{23}$$

In the case of Voigt model, the following relationship is well known

$$\tan \delta = \omega\tau \tag{24}$$

We obtain the friction length in the following form by substituting Eq. 23 and 24 into Eq. 22:

$$L_0 = (\mu_s - \mu_k - \mu_\delta)\, W/E - (v / \omega\pi) \ln \{(\mu_s - \mu_k) / \mu_\delta\} \ln R \tag{25}$$

Wear Equation

The cross-sectional area S of worn blade edges in Fig. 2 is $S = zh/2 = h^2/2\sin\theta\cos\theta$. Using Eq. 5 this leads to the following equation:

$$dS = h\, dh / \sin\theta \cos\theta = \alpha\, dl \tag{26}$$

$$S = \int \alpha\, d\, l = \alpha\, l = (u^2 / N_0 L_0)\, l \tag{27}$$

Substituting Eq. 11 and 25 into Eq. 27, the cross-sectional area of worn blade edge is given by

$$1/S \propto \frac{1}{u^2 l \mu^m W^{0.47m}} \left\{ \frac{(\mu_s - \mu_k - \mu_\delta)W}{E} - \left(\frac{\nu}{\omega\pi} \right) \ln \frac{\mu_s - \mu_k}{\mu_\delta} \ln R \right\} \quad (28)$$

Experimental

The cleaning blades made of thermohardened polyurethane rubber were studied. The specifications of the cleaning blades used are shown in Table 1.

The rebound resilience was measured by using Lüpke type testing apparatus. The rebound resilience is defined as the ratio of the energy after rebound to that before rebound when a pendulum having a spherical collision surface impacts a test sample. The rebound resilience of polyurethane strongly depends on temperature as shown in Table 1.

A 60 copies per minute copying machine was used as experimental apparatus. The photoconductive drum was kept at 30 °C with a heater. The development method was Micro-Toning system, and toner was styrene-acrylic resin based toner in average diameter of 11μm.

Table 1. Specification of Cleaning Blade Samples

Sample No.		Rebound Resilience 20°C	25°C	30°C
1	×	27	37	45
2	✳	27	37	46
3	□	39	50	57
4	○	51	59	64
5	△	58	65	71
6	◇	66	71	74
7	+	64	71	76
8		41	54	61

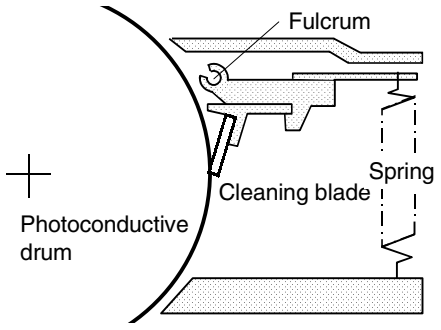

Figure 5. Blade cleaning apparatus

An illustration of the blade cleaning method is shown in Fig. 5. The main cleaning specifications were as follows:

- Cleaning method: Leading type
- Free length of blade: 9 mm
- Thickness of blade: 2 mm
- Contact line pressure: 1.8 g/mm
- Contact angle: 16°
- Diameter of photoconductive drum: 100 mm
- Photoconductor: Se alloy (surface roughness: 0.11 μm)
- Process speed: 382 mm/sec

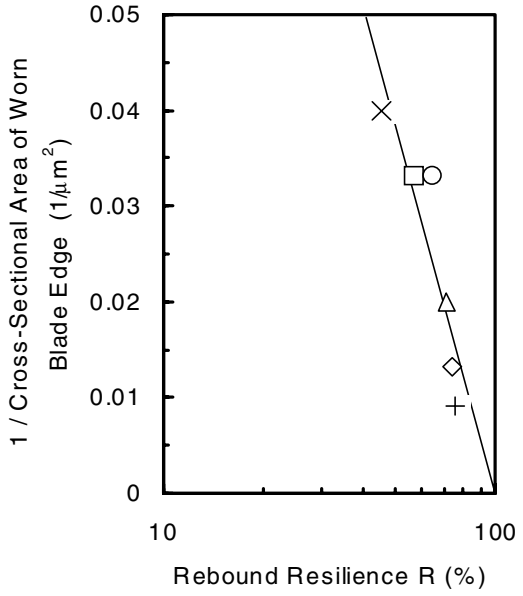

Figure 6. Cross-sectional area of worn blade edges as a function of rebound resilience after 3 hours operations under accelerated wear experiment. Solid line is a least square fit to Eq. 29.

Wear Experiment

The wear characteristics of the cleaning blades were investigated by accelerated wear experiment. The contact line pressure is increased by 40% up to 2.5 g/mm. The coefficient of friction is increased by 60% by using a mirror surface photoconductive drum. Blade edges are worn for 3 hours for samples No.1–No.7 indicated in Table 1. The reciprocal of cross-sectional area of worn blade edges as a function of the rebound resilience (at 30 °C) is shown in Fig. 6. The solid line is obtained by a least squares fit of the data to the following simplified form of Eq. 28,

$$1/S = C_1 - C_2 \ln R \quad (29)$$

C_1 and C_2 are determined to be $-0.0002\ \mu m^{-2}$ and $-0.0556\ \mu m^{-2}$, respectively. The close agreement between the theory and the observation is seen in Fig. 6. C_1 can be neglected and it means $L_{sl} >> L_{st}$ below R of 75%. Therefore, Eq. 28 reduces to the following equations:

$$1/S = \frac{C' \nu \ln R}{l \mu^m W^{0.47m}} \quad (30)$$

where C' is a constant. The number of copies N is proportional to the sliding. Therefore Eq. 30 can be changed into the following equation:

$$N = \frac{C'' \nu S \ln R}{\mu^m W^{0.47m}} \tag{31}$$

Cleaning Performance

Using a 60 cpm copying machines at room temperature, the cleaning performance of blades was evaluated by the number of copies made before a black stripe appeared on a copy. The temperature of the cleaning blade under experiment was measured as about 30°C. One cycle of copy mode per 24 hours was as follows:

- continuous 1.5 K copies
- 1.5 K copies made in 6 copies intervals
  - (Both of these were repeated 6 times)
- 1.5 K copies made with 1 copy/pause mode.

The cleaning performance of samples shown in Table 1 was evaluated. The relationships between the cleaning performance and hardness, tear strength, 300% modulus and Young's modulus were considered. However, the authors did not find significant correlation regarding those specifications.

The cleaning performance, i.e. the relationship between the number of copies made before cleaning failure and rebound resilience (at 30 °C) is shown in Fig. 7. The peak of the cleaning performance was noted at about R = 50%. Above this value the cleaning performance declined as R increased. Below this value the cleaning performance was extremely low. Because ν, S, μ and W are fixed in this experiment, Eq. 31 can be simplified as,

$$N = C \ln R \tag{32}$$

The solid curve in Fig. 7 is obtained from a least square fit of the data to Eq. 32.

The nip width for a new cleaning blade is about 20 μm. When the nip width of the worn-out cleaning blades becomes 40-50 μm, cleaning failure results. We assume that the cleaning failure occurs when the cross-sectional area of worn blade nips reaches a limited value S_o.

Effect of Weight and Friction Coefficient on Wear

For a comparison of experimental results in Fig. 6 (wear experiment) and Fig. 7 (cleaning performance) of the same blade sample, v and ln R in Eq. 30 remain constant. Therefore, it reduces to,

$$S = C L \mu^m W^{0.47m} \tag{33}$$

where L is the sliding distance calculated in terms of hours.

The L for the wear experiment is fixed at 3 hours. The friction coefficient is increased by 60% and the contact like pressure is increased by 40%. The cross-sectional area of cleaning blade of sample No. 3 in Fig. 7 was 55 μm^2.

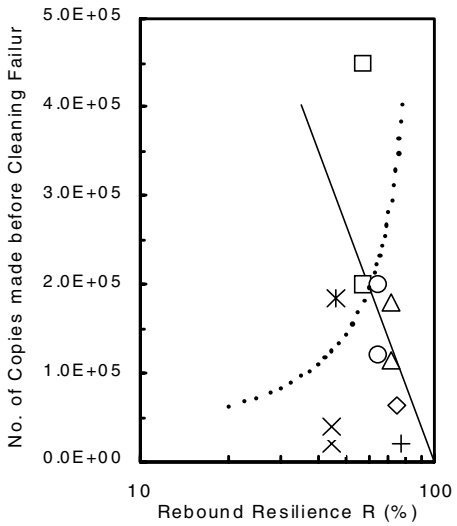

Figure 7. The number of copies made before the cleaning failure as a function of rebound resilience R using 60 cpm copying machines. Solid curve is a least square fit of data to Eq. 32. Dotted curve is the cleaning ability calculated from Eq. 36.

Denoting the friction coefficient of cleaning performance by $\boldsymbol{a}$, the pressure by $\boldsymbol{b}$, cross-sectional areas in the wear experiment by S_{aw} and sliding distance in the cleaning performance experiment by L_{nc}, the following equation is obtained from Eq. 30 and 31,

$$\frac{3\times(1.6\boldsymbol{a})^m(1.4\boldsymbol{b})^{0.47m}}{S_{aw}} = \frac{L_{nc}(\boldsymbol{a})^m(\boldsymbol{b})^{0.47m}}{55} \tag{34}$$

Therefore, the exponent m can be expressed as follows:

$$m = 3.67 \log \frac{L_{nc} S_{aw}}{165} \tag{35}$$

L_{nc} (h) is calculated from the number of copies in Fig. 7 by $L_{nc} = N$(copies) × 24(h)/16.5K (copies/day). Some calculated results of m are as follows:

Sample No.	N(copies)	m
No.3	200k	6.3
No.3	450k	7.6
No.4	120k	5.5
No.4	200k	6.3
No.5	110k	6.2
No.5	120k	6.3

The m of 6.5 at 25 °C was observed as shown in Fig. 4. The close agreement between the theory and the observation strongly suggests that the wear mechanism of rubber is fatigue destruction.

Cleaning Ability

Cleaning ability was evaluated by the number of copies made before cleaning failure occurred under severe

condition for cleaning blades. The 60 cpm copier was placed in a 10 °C and 15%RH environment. The temperature of the cleaning blades under experiment was measured as about 20 °C. A photoconductive drum with a mirror-quality surface was used. The copy mode was as follows: 100 copies of 6% black and white chart, followed by continuous copies of white chart until cleaning failures occurred.

Honda observed the behavior of toner in the neighborhood of the cleaning blade edge through high magnification CCD camera installed inside the glass based photoconductive drum[2]. He observed that toner particles blocked by the blade accumulate to form a pool of toner. This toner pool is made up of toner particles and surface treatment agent particles left almost unmoved, that is, a layer causing slipping with respect to the movement of the photoconductive surface. He called this the static toner region. It was found that in the static toner region, the nearer to the blade edge, the smaller the diameter of toner particles.

The blade nip and the static toner region move together with photoreceptor layer during the stick process according to the stick-slip model shown in Fig. 1. Therefore, toner particles cannot pass through the blade nip during the stick process. However, during the slip process, the blade forces remaining toner particles to move against rotating direction of photoconductive drum. It encounters greater possibility of toner particles going through blade nip during the slip process. Therefore, the cleaning ability is inversely proportional to the friction length.

$$\text{Cleaning ability} \propto 1 / L_0 \propto -1 / \ln R \qquad (36)$$

As shown in Fig. 8, the close agreement between Eq. 36 and the observation was confirmed. This model can be applied to explain the reason why the cleaning performance was extremely low below 50% of R as shown in Fig. 7.

Conclusions

We have examined the general profile of the cleaning performance (cleaning ability and lifetime of cleaning blades) in terms of tribology and rheology. The cleaning performance is closely related to the stick-slip behavior of the blade edges. This study has made it clear that the wear mechanism is fatigue destruction and toner particles go through blade nip during the slip process.

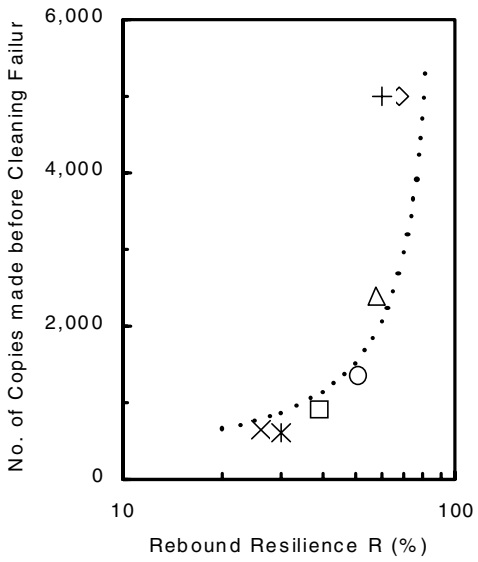

Figure 8. The number of copies made before the cleaning failure as a function of rebound resilience R under accelerated cleaning performance experiment. Dotted curve is cleaning ability calculated from Eq. 36.

Acknowledgments

We would like to express our deepest gratitude for the advice and cooperation of Mr. K. Kubota of Hokushin Corporation, and to their colleagues K. Tange, K. Matsushita and S. Hirota for their contribution to this study. The authors would like to acknowledge Dr. Inan Chen who reviewed this article and provided valuable suggestions.

References

1. Kuniki Seino, Keigo Tange, Shizuo Yuge and Masao Uemura, *Proc. IS&T's NIP13*, pg. 59 (1997).
2. M. Honda, H. Murasaki, *Electrophotography (Japanese Society Journal*, **34**, pg. 419 (1995).

Biography

Kuniki Seino received his M.S. degree in Physics in 1967 and a D.Sc. in Physics in 1972 from the Kwansei Gakuin University in Japan. He joined Minolta Co. Ltd., in 1967, where he has been engaged in research on photoreceptors and electrophotographic imaging processes. From 1991 to 1996, he managed the development of analog and digital copying machines including full color equipment. He is Senior Advisor for Imaging Technology to Minolta Co., Ltd. He is a member of the IS&T and the Imaging Society of Japan.